

This is the accepted manuscript made available via CHORUS. The article has been published as:

# Structure of $^{78}\text{Ni}$ from First-Principles Computations

G. Hagen, G. R. Jansen, and T. Papenbrock

Phys. Rev. Lett. **117**, 172501 — Published 17 October 2016

DOI: [10.1103/PhysRevLett.117.172501](https://doi.org/10.1103/PhysRevLett.117.172501)

# Structure of $^{78}\text{Ni}$ from first principles computations\*

G. Hagen,<sup>1,2</sup> G. R. Jansen,<sup>3,1</sup> and T. Papenbrock<sup>1,2</sup>

<sup>1</sup>*Physics Division, Oak Ridge National Laboratory, Oak Ridge, TN 37831, USA*

<sup>2</sup>*Department of Physics and Astronomy, University of Tennessee, Knoxville, TN 37996, USA*

<sup>3</sup>*National Center for Computational Sciences, Oak Ridge National Laboratory, Oak Ridge, TN 37831, USA*

Doubly magic nuclei have a simple structure and are the cornerstones for entire regions of the nuclear chart. Theoretical insights into the supposedly doubly magic  $^{78}\text{Ni}$  and its neighbors are challenging because of the extreme neutron-to-proton ratio and the proximity of the continuum. We predict the  $J^\pi = 2_1^+$  state in  $^{78}\text{Ni}$  from a correlation with the  $J^\pi = 2_1^+$  state in  $^{48}\text{Ca}$  using chiral nucleon-nucleon and three-nucleon interactions. Our results confirm that  $^{78}\text{Ni}$  is doubly magic, and the predicted low-lying states of  $^{79,80}\text{Ni}$  open the way for shell-model studies of many more rare isotopes.

*Introduction* – Doubly magic nuclei, i.e. nuclei with closed proton and neutron shells, play a most important role in nuclear physics [1]. They are more strongly bound than their neighbors, exhibit simple regular patterns, and are the cornerstones for our understanding of nuclear structure in entire regions of the Segré chart. In recent years, experiments and theory have made considerable progress in uncovering the evolution of shell structure in rare isotopes of oxygen [2–12], calcium [13–20], and tin [21–23].

The supposedly doubly magic nucleus  $^{78}\text{Ni}$  (with neutron number 50 and proton number 28) has been the focus of considerable experimental and theoretical efforts [24–30]. This nucleus is also of astrophysical relevance because it is in the region of the  $r$ -process path. Reliable theoretical predictions for  $^{78}\text{Ni}$  and its neighbors are challenging [31, 32], because of the extreme neutron-to-proton ratio and the proximity to the neutron dripline. The large isospin brings to the fore smaller aspects of the nuclear interaction that are poorly constrained in  $\beta$  stable nuclei, while for weakly bound and unbound nuclear states it is necessary to include coupling to the particle continuum. We address these challenges as follows: We employ a set of interactions [33, 34] from chiral effective field theory (EFT) [35–37]. These interactions consist of nucleon-nucleon ( $NN$ ) and three-nucleon forces (3NFs) [38, 39]. They reproduce properties of nuclei with mass numbers  $A = 2, 3, 4$  nuclei well, but differ in binding energies, radii, and spectra of medium-mass nuclei [40]. We include continuum physics by employing the Berggren basis [41–43] which treats bound-,

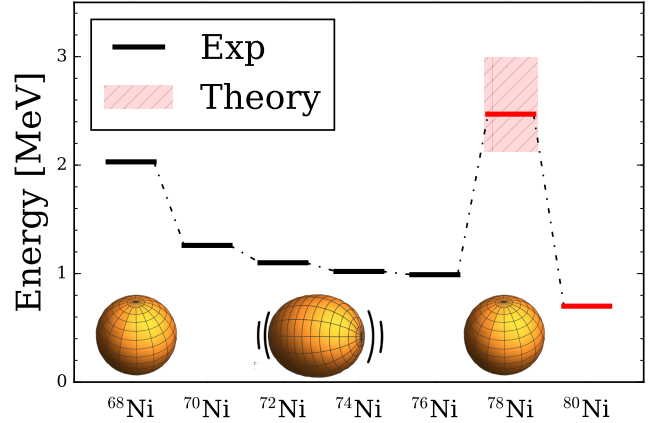


FIG. 1. (Color online) Energy of the  $2_1^+$  state in neutron-rich nickel isotopes for  $^{68-76}\text{Ni}$  from data (black horizontal lines) and for  $^{78,80}\text{Ni}$  from first-principles computations (red horizontal lines) based on the chiral interaction “1.8/2.0 (EM)” of Ref. [33]. The red shaded area for  $^{78}\text{Ni}$  shows the predicted range for the  $2_1^+$  state based on a correlation between the  $2_1^+$  in  $^{48}\text{Ca}$  and  $^{78}\text{Ni}$  using a family of chiral interactions (see text and Fig. 2 for details).

resonant-, and non-resonant scattering states on equal footing. The Berggren basis has been extensively used in the Gamow-shell-model and coupled-cluster computations of weakly bound and unbound nuclear states, see for example [44–46]. Finally, using these ingredients we solve for the structure of  $^{78}\text{Ni}$  and its neighbors using coupled-cluster theory [47–56], see Refs. [57, 58] for recent reviews. For the computation of  $J^\pi = 2_1^+$  excited states in  $^{48}\text{Ca}$  and  $^{78}\text{Ni}$  we use an implementation of the equation-of-motion (EOM) coupled-cluster method that properly accounts for two-particle-two-hole ( $2p-2h$ ) excitations.

As a key indicator of the  $^{78}\text{Ni}$  structure, we focus on the energy of the first excited  $J^\pi = 2_1^+$  state. This  $2_1^+$  state is at about 1 MeV of excitation energy in  $^{70,72,74,76}\text{Ni}$ , reflecting a softness regarding (a collective) quadrupole vibration. In contrast to these semi magic nuclei, the nucleus  $^{68}\text{Ni}$  exhibits a soft subshell closure (at neutron

\* This manuscript has been authored by UT-Battelle, LLC under Contract No. DE-AC05-00OR22725 with the U.S. Department of Energy. The United States Government retains and the publisher, by accepting the article for publication, acknowledges that the United States Government retains a non-exclusive, paid-up, irrevocable, world-wide license to publish or reproduce the published form of this manuscript, or allow others to do so, for United States Government purposes. The Department of Energy will provide public access to these results of federally sponsored research in accordance with the DOE Public Access Plan. (<http://energy.gov/downloads/doe-public-access-plan>).

number 40) [59, 60], and its  $2_1^+$  state is at about 2 MeV of excitation energy. This situation is illustrated in Fig. 1, with experimentally known  $2_1^+$  levels shown as black bars and the computed energies of the  $2_1^+$  states in  $^{78,80}\text{Ni}$  from this Letter. For  $^{78}\text{Ni}$  the red shaded area gives the predicted range for the  $2_1^+$  state obtained by correlating relevant observables; details are given below. The predicted range for the  $2_1^+$  state in  $^{78}\text{Ni}$  is considerably higher than for its neighbors – indicating that this nucleus is doubly magic. This is the main result of this Letter. The red bar marks the result obtained with the interaction “1.8/2.0(EM)” from Ref. [33], which is singled out because it accurately reproduces the binding energy of  $^{78}\text{Ni}$ , as well as the nuclei  $^4\text{He}$ ,  $^{16}\text{O}$ , and  $^{40,48}\text{Ca}$ .

This Letter is organized as follows. We briefly summarize the Hamiltonian and model-spaces that are input to the calculations of neutron-rich nickel isotopes. We discuss an implementation of three-particle-three-hole corrections to coupled-cluster computations of excited states. Using these theoretical ingredients we compute the first  $2_1^+$  state in the doubly magic  $^{48}\text{Ca}$  and in  $^{78}\text{Ni}$  from a family of chiral  $NN$  and  $3\text{NFs}$ . From an observed correlation between the energies of the  $2_1^+$  states in  $^{48}\text{Ca}$  and  $^{78}\text{Ni}$  we obtain a range for the latter. We discuss the relevance of  $2p$ - $2h$  excitations in this state. We also give predictions for other low-lying states in  $^{78}\text{Ni}$ . Finally we focus on the neighbors of  $^{78}\text{Ni}$  and present predictions for low-lying states in  $^{77,79,80}\text{Ni}$ .

*Hamiltonian and model-space* – Our coupled-cluster calculations start from the intrinsic Hamiltonian

$$\hat{H} = \sum_{i < j} \left( \frac{(\mathbf{p}_i - \mathbf{p}_j)^2}{2mA} + \hat{V}_{NN}^{(i,j)} \right) + \sum_{i < j < k} \hat{V}_{3N}^{(i,j,k)}. \quad (1)$$

We compute the Hamiltonian (1) using interactions from Refs. [33, 34]. The interactions of Ref. [33] are based on similarity-renormalization-group (SRG) [61] transformations of  $NN$  interactions from chiral EFT augmented with leading  $3\text{NFs}$  from chiral EFT. Here, the low-energy constants of the  $3\text{NFs}$  are adjusted to data from nuclei with mass numbers  $A = 3, 4$ . These interactions yield saturation points for nuclear matter around the empirical value [33], and they yield radii and binding energies in calcium isotopes scattered around data [40]. The interaction  $\text{NNLO}_{\text{sat}}$  of Ref. [34] by construction yields accurate radii and binding energies in light nuclei and isotopes of oxygen. It extrapolates well to calcium isotopes [40] and  $^{56}\text{Ni}$  [62], and within uncertainties reproduces the empirical saturation point in symmetric nuclear matter. We employ these interactions to study systematic sensitivities because a full-fledged propagation of uncertainties is not yet possible [63]. The five interactions used in this Letter have different cutoffs and three different sets of pion-nucleon constants, i.e. they also differ in the long-range part of the nuclear interaction. They are truly different parametrizations of chiral EFTs that de-

scribe  $A = 2, 3, 4$  nuclei about equally well, but differ in medium-mass nuclei [40], see also Ref. [64].

We use a Hartree-Fock basis constructed from a harmonic oscillator basis of up to 15 major oscillator shells. To compute weakly bound and unbound states in  $^{79}\text{Ni}$  we construct a Gamow-Hartree-Fock basis [46, 65] by including a Berggren basis for relevant partial waves and follow Ref. [62] for inclusion of  $3\text{NFs}$ . For  $^{48}\text{Ca}$  we use the same model-spaces that were employed in Ref. [40], while for the neutron-rich nickel isotopes we perform the calculations at the oscillator frequency  $\hbar\omega = 16$  MeV which yields the minimum in energy for the largest model-space that we consider. We use the normal-ordered two-body approximation [66–68] for the  $3\text{NF}$  with the additional three-body energy cut  $E_{3\text{max}} = N_1 + N_2 + N_3 \leq 16$ . Here  $N_i = 2n_i + l_i$  refers to the oscillator shell of the  $i^{\text{th}}$  particle.

*Method* – We employ the coupled-cluster singles-doubles (CCSD) approximation in an angular momentum coupled representation and compute the similarity-transformed Hamiltonian  $\bar{H}$  (see Refs. [58, 69] for details). We include triple excitations perturbatively using the  $\Lambda$ -CCSD(T) method [70] for the computation of the ground-state energy. The excited  $2_1^+$  state is computed with the EOM coupled-cluster method in the EOM-CCSD [71] and EOM-CCSD(T) approximations [72]. EOM-CCSD has been shown to be accurate for states that are dominated by  $1p$ - $1h$  excitations [57]. In this Letter we go beyond the standard EOM-CCSD approach and include corrections from  $3p$ - $3h$  excitations perturbatively using the EOM-CCSD(T) approach. EOM-CCSD(T) capture the dominant  $2p$ - $2h$  excitations in the computation of the  $2_1^+$  state in  $^{48}\text{Ca}$  and  $^{78}\text{Ni}$ . This method generalizes the  $\Lambda$ -CCSD(T) approach for the ground-state energy and requires the solution of both the left and right EOM-CCSD eigenvalue problem, with a non-iterative  $3p$ - $3h$  correction computed perturbatively. The computational cost is considerably larger than for  $\Lambda$ -CCSD(T) since we are considering a non-scalar excitation. In quantum chemistry applications, EOM-CCSD(T) is an economical and accurate correction to EOM-CCSD [73]. Excited states in neighboring nuclei  $^{77,79,80}\text{Ni}$  are computed as generalized  $mp$ - $nh$  excited states [69, 74, 75] of  $\bar{H}$ . Details of this approach are presented in the review [58] and in the supplementary information of Ref. [40].

*Results* – To probe the quality of the EOM-CCSD(T) approximation, and for a comparison with data, we also compute the  $2_1^+$  excited state in  $^{48}\text{Ca}$ . For the computation of the  $2_1^+$  state in  $^{78}\text{Ni}$ , we employ the same interactions but choose lower model space frequencies to minimize the ground-state energies.

Figure 2 shows that the excitation energy of the  $2_1^+$  state in  $^{48}\text{Ca}$  and  $^{78}\text{Ni}$  are strongly correlated. The error bars on the individual data points estimate uncertainties from the method and model-space truncation. We estimate the model-space uncertainty from enlarging the

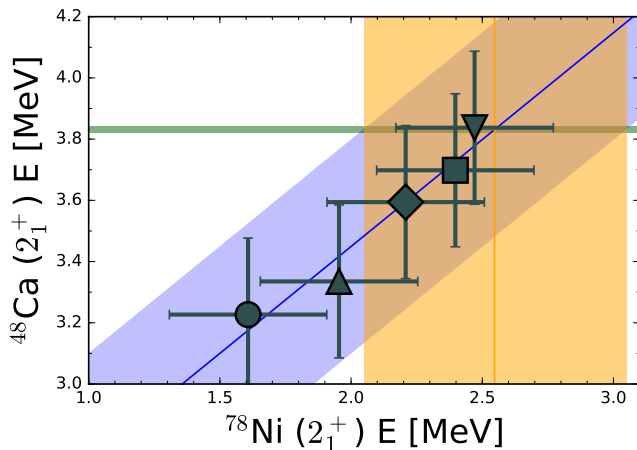


FIG. 2. (Color online) Correlation between the energies of the  $2_1^+$  excited state in  $^{48}\text{Ca}$  and  $^{78}\text{Ni}$ , obtained from the interactions  $\text{NNLO}_{\text{sat}}$  (circle), “2.0/2.0 (PWA)” (square), “2.0/2.0 (EM)” (diamond), “2.2/2.0 (EM)” (triangle up), and “1.8/2.0 (EM)” (triangle down). The error bars estimate uncertainties from enlarging the model space from  $N = 12$  to  $N = 14$ . The thin horizontal line marks the known energy of the  $2_1^+$  state in  $^{48}\text{Ca}$ .

model space from  $N = 12$  to  $N = 14$  which is less than 200 keV for all employed interactions. For the method we include 10% of the triples correlation energy as an uncertainty estimate. We take the average from all interactions and give a combined uncertainty on the  $2_1^+$  state in  $^{48}\text{Ca}$  and  $^{78}\text{Ni}$ . A linear fit to the data points, and an encompassing diagonal uncertainty band is also shown. The thin horizontal line marks the known energy of the  $2_1^+$  state in  $^{48}\text{Ca}$ , and its intersection with the diagonal band projects out our theoretical estimate  $2.1 \text{ MeV} \lesssim E(2_1^+) \lesssim 3.1 \text{ MeV}$  for the energy of the  $2_1^+$  state in  $^{78}\text{Ni}$ . This band is also shown in Fig. 1. We note that two of the five employed interactions reproduce the energy of the  $2_1^+$  state in  $^{48}\text{Ca}$  within uncertainties. The interaction  $\text{NNLO}_{\text{sat}}$ , which accurately reproduces charge radii in  $^{48}\text{Ca}$ , yields an excitation energy that is too low. We also note that the origin of the correlation between the  $2_1^+$  states in  $^{48}\text{Ca}$  and  $^{78}\text{Ni}$  depicted in Fig. 2 is not understood theoretically. While several such correlations have been reported (and exploited) in the literature, see, e.g., Refs. [40, 76, 77], only few have been understood [78]. In the supplemental material [79] we show that the correlation reported in Fig. 2 is nontrivial. The spectroscopy of  $^{78}\text{Ni}$  was recently measured at RIBF, RIKEN [80], and it will be interesting to compare our theoretical result with data.

For  $^{78}\text{Ni}$ , the convergence of the ground-state energy with respect to the size of the model space is slow for most of the employed interactions, and we are only able to achieve convergence for the softest interaction “1.8/2.0 (EM)” of Ref. [33]. For this interaction the com-

puted binding energy is 637(4) MeV which agrees with the value 641 MeV extracted from systematic trends. The  $E_{3\text{max}}$  truncation used for the 3NF is the dominant uncertainty, and the estimated error of 4 MeV comes from increasing  $E_{3\text{max}}$  from 14 to 16 [79]. We note that the convergence is improved for energy differences. Figure 3 shows the convergence of the energy of the  $2_1^+$  state in  $^{48}\text{Ca}$  and  $^{78}\text{Ni}$  with increasing size of the model space, obtained for the interaction “1.8/2.0 (EM)”. The convergence is qualitatively similar for the other interactions, and the difference between the  $N = 12$  and  $N = 14$  spaces entered the uncertainties presented in Fig. 2. Further details on the convergence are presented in the supplemental material [79].

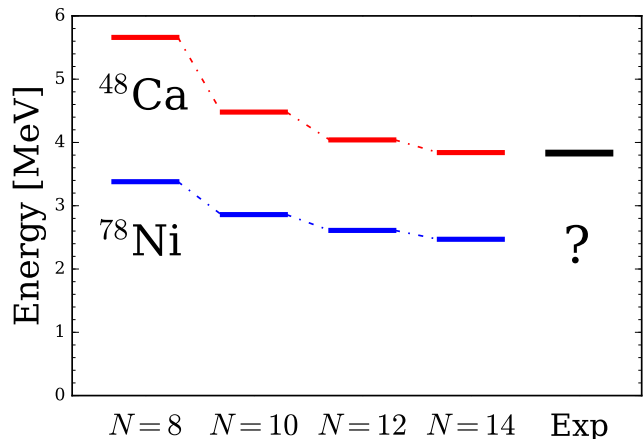


FIG. 3. (Color online) Convergence of the first  $2_1^+$  excited state of  $^{48}\text{Ca}$  and  $^{78}\text{Ni}$  with increasing model-space size and compared to data for the interaction “1.8/2.0 (EM)” of Ref. [33].

We note that the interaction “1.8/2.0 (EM)” describes the  $2_1^+$  state in  $^{48}\text{Ca}$  and the binding energies for a variety of nuclei remarkably well. For example, the computed binding energies for  $^4\text{He}$ ,  $^{16}\text{O}$  and  $^{40,48}\text{Ca}$  are 28.2 MeV, 128 MeV, 348 MeV, and 419 MeV, respectively; they are close to the corresponding experimental binding energies of 28.2 MeV, 128 MeV, 342 MeV, and 416 MeV.

Let us discuss the effect of  $2p\text{-}2h$  excitations in the  $2_1^+$  excited state of  $^{48}\text{Ca}$  and  $^{78}\text{Ni}$ . Table I shows results for this state using the EOM-CCS, EOM-CCSD and EOM-CCSD(T) approximations for the interactions used in this work. We find that the inclusion of perturbative  $3p\text{-}3h$  excitations in EOM-CCSD(T) reduces the excitation energy by 1-2 MeV for all interactions when compared to the corresponding EOM-CCSD results. The triples corrections for the  $2_1^+$  state in both  $^{48}\text{Ca}$  and in  $^{78}\text{Ni}$  amounts to about 20% of the EOM-CCSD correlation energy (defined as the difference between the EOM-CCS and EOM-CCSD excitation energies). In coupled cluster theory, one could conservatively assume that  $4p\text{-}4h$  contributions are again of the order of 20% of the

3p-3h correction, yielding uncertainty estimates that are within the uncertainties shown in Fig. 2. We note that the role of 3p-3h excitations in the computation of the  $2_1^+$  state in both  $^{48}\text{Ca}$  and in  $^{78}\text{Ni}$  is considerably larger than the role of 3p-3h excitations in the ground-state. For the ground-state of closed (sub-)shell nuclei the triples correlation energy typically amounts to about 10% of the CCSD correlation energy, see Ref. [81] for an example. We also note that the role of correlations beyond 1p-1h is larger than in RPA calculations based on Skyrme-Hartree-Fock because those yield much less correlated wave functions (*cf.* Ref. [82] for a recent application to nickel isotopes.)

Interaction	$^{48}\text{Ca}$			$^{78}\text{Ni}$		
	1p-1h	2p-2h	3p-3h	1p-1h	2p-2h	3p-3h
1.8/2.0 (EM)	10.5	4.9	3.8	8.5	3.5	2.5
2.0/2.0 (EM)	11.3	4.9	3.6	9.1	3.4	2.2
2.2/2.0 (EM)	12.0	4.8	3.3	9.5	3.4	2.0
2.0/2.0 (PWA)	12.0	5.2	3.7	9.8	3.8	2.4
NNLO <sub>sat</sub>	14.8	5.3	3.2	12.2	3.8	1.6

TABLE I. Results for the excitation energy (in MeV) of the  $2_1^+$  state in  $^{48}\text{Ca}$  and  $^{78}\text{Ni}$  computed in the EOM-CCS (denoted by 1p-1h), EOM-CCSD (denoted by 2p-2h) and EOM-CCSD(T) (denoted by 3p-3h) approximations. The interactions labeled (EM) and (PWA) are taken from Ref. [33] and NNLO<sub>sat</sub> is from Ref. [34].

Our analysis shows that 2p-2h excitations are significant for the  $2_1^+$  state in  $^{48}\text{Ca}$  and  $^{78}\text{Ni}$ , and that a precise description of this state therefore requires EOM-CCSD(T). This finding is somewhat surprising, because the collective  $2_1^+$  state is usually thought of as a coherent superposition of 1p-1h excitations [83]. However, a simple shell-model argument suggests that 2p-2h excitations should yield significant corrections. In the doubly-magic  $^{48}\text{Ca}$  for instance, no 1p-1h excitations of protons near the Fermi surface can generate a  $2^+$  state, as one need at least 2p-2h excitations from the *sd* shell to the *pf* shell to yield a  $2^+$  state. Following the same reasoning, a computation of the electric quadrupole transition in  $^{48}\text{Ca}$  will have significant 2p-2h contributions since this observable measures mostly the excitations of protons. Similarly, we find that for  $^{78}\text{Ni}$  2p-2h excitations of neutrons near the Fermi surface have significant contributions to the low-lying  $2_1^+$  state. In the naive shell-model picture the  $g_{9/2}$  orbital is the last filled neutron shell with  $s_{1/2}$ ,  $d_{5/2}$ ,  $d_{3/2}$ ,  $g_{7/2}$  shells being the next unoccupied orbitals closest to the Fermi surface. A  $2^+$  state near the Fermi surface can be generated via 1p-1h excitations of neutrons from the  $g_{9/2}$  to the  $d_{5/2}$ ,  $g_{7/2}$  orbitals, but 2p-2h excitations are necessary to utilize the low-lying  $s_{1/2}$  and  $d_{3/2}$  orbitals. As shown in Tab. I the effect of 2p-2h excitations from the  $g_{9/2}$  to the  $s_{1/2}$  and  $d_{3/2}$  orbitals is significant in the  $2^+$  state of  $^{78}\text{Ni}$ . As we will see below the  $1/2^+$  state is actually the lowest state in  $^{79}\text{Ni}$ .

Shell closures manifest themselves in several observables. Besides the energy of the  $2_1^+$  state, separation energies also yield valuable information. For the computation of other low-lying states in  $^{78}\text{Ni}$  and its neighbors  $^{77,79,80}\text{Ni}$ , we limit ourselves to the “1.8/2.0 (EM)” interaction because this interaction yields converged results with respect to the model space and accurate energies. For  $^{79}\text{Ni}$ , we employed a Berggren basis for the  $s_{1/2}$ ,  $d_{5/2}$  and  $d_{3/2}$  partial waves because of the proximity of the continuum. For the  $g_{7/2}$  partial wave we use the harmonic-oscillator basis, because the large centrifugal barrier reduces the impact of the coupling to the continuum. The resulting spectra are shown in Fig. 4 relative to the ground-state energy of  $^{78}\text{Ni}$ . For  $^{78}\text{Ni}$  we predict low-lying  $1_1^+$ ,  $3_1^+$ ,  $4_1^+$  excited states all below the neutron-emission threshold. The ratio of the excited  $4_1^+$  state with the  $2_1^+$  state is 1.2, which is consistent with  $^{78}\text{Ni}$  being a doubly magic nucleus. Due to the high computational cost the  $1_1^+$ ,  $3_1^+$ ,  $4_1^+$  excited states in  $^{78}\text{Ni}$  were computed with  $N = 12$ ; the triples correlation energy for the  $4_1^+$  state was well converged for  $N = 10$ . The theoretical result for the neutron-separation energies in  $^{78,79}\text{Ni}$  are  $S_n \approx 4.5$  MeV and  $S_n \approx 1$  MeV, respectively, which are consistent with 5450(950) keV and 1650(1130) keV from systematics [84]. For  $^{79}\text{Ni}$  we find that the inclusion of the continuum impacts the level ordering and lowers the  $1/2^+$  state by about 1 MeV, the  $5/2^+$  state by about 0.5 MeV, and the unbound  $3/2^+$  state by about 0.7 MeV, as compared to a calculation in the harmonic oscillator basis.

The  $1/2^+$  ground-state of  $^{79}\text{Ni}$  is quasi-degenerate with the  $5/2^+$  state. This finding mirrors the results of Refs. [15, 62, 85], where the inclusion of continuum effects also impacted the energies and level ordering of unbound states in the neutron-rich calcium isotopes  $^{53,55,61}\text{Ca}$ . The ground-state of  $^{80}\text{Ni}$  is bound by 2 MeV with respect to  $^{78}\text{Ni}$ , thereby setting the neutron dripline beyond  $^{80}\text{Ni}$ . This is consistent with mean-field surveys [86]. The two-neutron separation  $S_{2n}(^{80}\text{Ni}) \approx 2$  MeV is significantly smaller than the estimate  $S_{2n}(^{78}\text{Ni}) = 8660(950)$  keV [84] – consistent with expectations for a doubly magic nucleus. The  $2_1^+$  state in  $^{80}\text{Ni}$  is computed to be 0.7 MeV above its ground state. The combined results of this study – a relatively high-lying  $2_1^+$  state in  $^{78}\text{Ni}$ , the marked difference of neutron-separation energies between  $^{79}\text{Ni}$  and  $^{78}\text{Ni}$ , and of two-neutron separation energies between  $^{80}\text{Ni}$  and  $^{78}\text{Ni}$ , respectively, indicate the strength of the shell closure at neutron number 50.

*Conclusions* – We presented first-principles computations of the structure of  $^{78}\text{Ni}$  and its neighbors. Correlating the  $2_1^+$  energies in  $^{78}\text{Ni}$  and  $^{48}\text{Ca}$  leads to the prediction  $2.1 \text{ MeV} \lesssim E(2_1^+) \lesssim 3.1 \text{ MeV}$  for the energy of the  $2_1^+$  state in  $^{78}\text{Ni}$ . Neutron separation energies and two-neutron separation energies confirm the picture of the shell closure at neutron number 50, and the theoretical results put the neutron dripline beyond  $^{80}\text{Ni}$ . We also

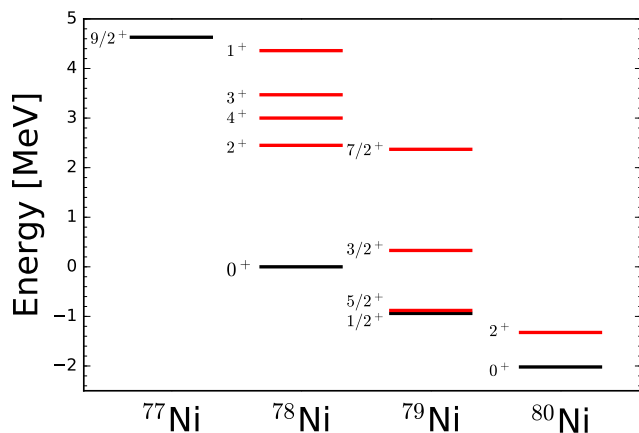


FIG. 4. (Color online) Low-lying states in  $^{77-80}\text{Ni}$  with respect to the ground-state of  $^{78}\text{Ni}$  computed with the interaction “1.8/2.0 (EM)” of Ref. [33]. The ground states are shown in black, while excited states are shown in red.

made predictions for low-lying states in  $^{77,78,79,80}\text{Ni}$  that can be confronted by experiment. As a useful theoretical tool, a relatively soft chiral interaction emerged as being in good agreement with binding energies and low-lying excitations from  $^4\text{He}$ , to  $^{16}\text{O}$ , to  $^{40,48}\text{Ca}$  to  $^{78}\text{Ni}$ . This study paves the way to theoretical predictions in heavy rare isotopes.

We thank Kai Hebeler for providing us with matrix elements in Jacobi coordinates for the three-nucleon interaction at next-to-next-to-leading order. This work was supported by the Office of Nuclear Physics, U.S. Department of Energy, under grants DE-FG02-96ER40963, DE-SC0008499 (NUCLEI SciDAC collaboration), and the Field Work Proposal ERKBP57 at Oak Ridge National Laboratory (ORNL). Computer time was provided by the Innovative and Novel Computational Impact on Theory and Experiment (INCITE) program. This research used resources of the Oak Ridge Leadership Computing Facility located at ORNL, which is supported by the Office of Science of the Department of Energy under Contract No. DE-AC05-00OR22725.

- 
- [1] M. G. Mayer and J. H. D. Jensen, *Elementary Theory of Nuclear Shell Structure* (John Wiley & Sons, New York, 1955).
  - [2] A. Volya and V. Zelevinsky, “Discrete and continuum spectra in the unified shell model approach,” *Phys. Rev. Lett.* **94**, 052501 (2005).
  - [3] C. R. Hoffman, T. Baumann, D. Bazin, J. Brown, G. Christian, P. A. DeYoung, J. E. Finck, N. Frank, J. Hinnefeld, R. Howes, P. Mears, E. Mosby, S. Mosby, J. Reith, B. Rizzo, W. F. Rogers, G. Peaslee, W. A. Peters, A. Schiller, M. J. Scott, S. L. Tabor, M. Thoennessen, P. J. Voss, and T. Williams, “Determination of

the  $N = 16$  Shell Closure at the Oxygen Drip Line,” *Phys. Rev. Lett.* **100**, 152502 (2008).

- [4] R. Kanungo, C. Nociforo, A. Prochazka, T. Aumann, D. Boutin, D. Cortina-Gil, B. Davids, M. Diakaki, F. Farinon, H. Geissel, R. Gernhäuser, J. Gerl, R. Janik, B. Jonson, B. Kindler, R. Knöbel, R. Krücken, M. Lantz, H. Lenske, Y. Litvinov, B. Lommel, K. Mahata, P. Maierbeck, A. Musumarra, T. Nilsson, T. Otsuka, C. Perro, C. Scheidenberger, B. Sitar, P. Strmen, B. Sun, I. Szarka, I. Tanihata, Y. Utsuno, H. Weick, and M. Winkler, “One-neutron removal measurement reveals  $^{24}\text{O}$  as a new doubly magic nucleus,” *Phys. Rev. Lett.* **102**, 152501 (2009).
- [5] C. R. Hoffman, T. Baumann, D. Bazin, J. Brown, G. Christian, D. H. Denby, P. A. DeYoung, J. E. Finck, N. Frank, J. Hinnefeld, S. Mosby, W. A. Peters, W. F. Rogers, A. Schiller, A. Spyrou, M. J. Scott, S. L. Tabor, M. Thoennessen, and P. Voss, “Evidence for a doubly magic  $^{24}\text{O}$ ,” *Phys. Lett. B* **672**, 17 – 21 (2009).
- [6] T. Otsuka, T. Suzuki, J. D. Holt, A. Schwenk, and Y. Akaishi, “Three-body forces and the limit of oxygen isotopes,” *Phys. Rev. Lett.* **105**, 032501 (2010).
- [7] R. Kanungo, A. Prochazka, M. Uchida, W. Horiuchi, G. Hagen, T. Papenbrock, C. Nociforo, T. Aumann, D. Boutin, D. Cortina-Gil, B. Davids, M. Diakaki, F. Farinon, H. Geissel, R. Gernhäuser, J. Gerl, R. Janik, Ø. Jensen, B. Jonson, B. Kindler, R. Knöbel, R. Krücken, M. Lantz, H. Lenske, Y. Litvinov, B. Lommel, K. Mahata, P. Maierbeck, A. Musumarra, T. Nilsson, C. Perro, C. Scheidenberger, B. Sitar, P. Strmen, B. Sun, Y. Suzuki, I. Szarka, I. Tanihata, H. Weick, and M. Winkler, “Exploring the anomaly in the interaction cross section and matter radius of  $^{23}\text{O}$ ,” *Phys. Rev. C* **84**, 061304 (2011).
- [8] E. Lunderberg, P. A. DeYoung, Z. Kohley, H. Attanayake, T. Baumann, D. Bazin, G. Christian, D. Divaratne, S. M. Grimes, A. Haagsma, J. E. Finck, N. Frank, B. Luther, S. Mosby, T. Nagi, G. F. Peaslee, A. Schiller, J. Snyder, A. Spyrou, M. J. Strongman, and M. Thoennessen, “Evidence for the ground-state resonance of  $^{26}\text{O}$ ,” *Phys. Rev. Lett.* **108**, 142503 (2012).
- [9] G. Hagen, M. Hjorth-Jensen, G. R. Jansen, R. Machleidt, and T. Papenbrock, “Continuum effects and three-nucleon forces in neutron-rich oxygen isotopes,” *Phys. Rev. Lett.* **108**, 242501 (2012).
- [10] H. Hergert, S. Binder, A. Calci, J. Langhammer, and R. Roth, “*Ab Initio* calculations of even oxygen isotopes with chiral two-plus-three-nucleon interactions,” *Phys. Rev. Lett.* **110**, 242501 (2013).
- [11] A. Cipollone, C. Barbieri, and P. Navrátil, “Isotopic chains around oxygen from evolved chiral two- and three-nucleon interactions,” *Phys. Rev. Lett.* **111**, 062501 (2013).
- [12] C. Caesar, J. Simonis, T. Adachi, Y. Aksyutina, J. Alcantara, S. Altstadt, H. Alvarez-Pol, N. Ashwood, T. Aumann, V. Avdeichikov, M. Barr, S. Beceiro, D. Bemmerer, J. Benlliure, C. A. Bertulani, K. Boretzky, M. J. G. Borge, G. Burgunder, M. Caamano, E. Casarejos, W. Catford, J. Cederkäll, S. Chakraborty, M. Chartier, L. Chulkov, D. Cortina-Gil, U. Datta Pramanik, P. Diaz Fernandez, I. Dillmann, Z. Elekes, J. Enders, O. Ershova, A. Estrade, F. Farinon, L. M. Fraile, M. Freer, M. Freudenberger, H. O. U. Fynbo, D. Galaviz, H. Geissel, R. Gernhäuser, P. Golubev, D. Gonzá-



- lez Diaz, J. Hagdahl, T. Heftrich, M. Heil, M. Heine, A. Heinz, A. Henriques, M. Holl, J. D. Holt, G. Ickert, A. Ignatov, B. Jakobsson, H. T. Johansson, B. Jonsson, N. Kalantar-Nayestanaki, R. Kanungo, A. Kelic-Heil, R. Knöbel, T. Kröll, R. Krücken, J. Kurcewicz, M. Labiche, C. Langer, T. Le Bleis, R. Lemmon, O. Lepyoshkina, S. Lindberg, J. Machado, J. Marganec, V. Maroussov, J. Menéndez, M. Mostazo, A. Movsesyan, A. Najafi, T. Nilsson, C. Nociforo, V. Panin, A. Perea, S. Pietri, R. Plag, A. Prochazka, A. Rahaman, G. Rastrepina, R. Reifarth, G. Ribeiro, M. V. Ricciardi, C. Rigollet, K. Riisager, M. Röder, D. Rossi, J. Sanchez del Rio, D. Savran, H. Scheit, A. Schwenk, H. Simon, O. Sorlin, V. Stoica, B. Streicher, J. Taylor, O. Tengblad, S. Terashima, R. Thies, Y. Togano, E. Uberseder, J. Van de Walle, P. Velho, V. Volkov, A. Wagner, F. Wamers, H. Weick, M. Weigand, C. Wheldon, G. Wilson, C. Wimmer, J. S. Winfield, P. Woods, D. Yakorev, M. V. Zhukov, A. Zilges, M. Zoric, and K. Zuber (R3B collaboration), “Beyond the neutron drip line: The unbound oxygen isotopes  $^{25}\text{O}$  and  $^{26}\text{O}$ ,” *Phys. Rev. C* **88**, 034313 (2013).
- [13] A. T. Gallant, J. C. Bale, T. Brunner, U. Chowdhury, S. Ettenauer, A. Lennarz, D. Robertson, V. V. Simon, A. Chaudhuri, J. D. Holt, A. A. Kwiatkowski, E. Manó, J. Menéndez, B. E. Schultz, M. C. Simon, C. Andreoiu, P. Delheij, M. R. Pearson, H. Savajols, A. Schwenk, and J. Dilling, “New precision mass measurements of neutron-rich calcium and potassium isotopes and three-nucleon forces,” *Phys. Rev. Lett.* **109**, 032506 (2012).
- [14] J. D. Holt, T. Otsuka, A. Schwenk, and T. Suzuki, “Three-body forces and shell structure in calcium isotopes,” *J. Phys. G: Nucl. Part. Phys.* **39**, 085111 (2012).
- [15] G. Hagen, M. Hjorth-Jensen, G. R. Jansen, R. Machleidt, and T. Papenbrock, “Evolution of shell structure in neutron-rich calcium isotopes,” *Phys. Rev. Lett.* **109**, 032502 (2012).
- [16] F. Wienholtz, D. Beck, K. Blaum, Ch. Borgmann, M. Breitenfeldt, R. B. Cakirli, S. George, F. Herfurth, J. D. Holt, M. Kowalska, S. Kreim, D. Lunney, V. Manea, J. Menendez, D. Neidherr, M. Rosenbusch, L. Schweikhard, A. Schwenk, J. Simonis, J. Stanja, R. N. Wolf, and K. Zuber, “Masses of exotic calcium isotopes pin down nuclear forces,” *Nature* **498**, 346–349 (2013).
- [17] D. Steppenbeck, S. Takeuchi, N. Aoi, P. Doornenbal, J. Lee, M. Matsushita, H. Wang, H. Baba, N. Fukuda, S. Go, M. Honma, K. Matsui, S. Michimasa, T. Motobayashi, D. Nishimura, T. Otsuka, H. Sakurai, Y. Shiga, P.-A. Söderström, T. Sumikama, H. Suzuki, R. Taniuchi, Y. Utsuno, J. J. Valiente-Dobón, and K. Yoneda, “Investigating the strength of the  $N = 34$  subshell closure in  $^{54}\text{Ca}$ ,” *J. Phys.: Conf. Ser.* **445**, 012012 (2013).
- [18] D. Steppenbeck, S. Takeuchi, N. Aoi, P. Doornenbal, M. Matsushita, H. Wang, H. Baba, N. Fukuda, S. Go, M. Honma, J. Lee, K. Matsui, S. Michimasa, T. Motobayashi, D. Nishimura, T. Otsuka, H. Sakurai, Y. Shiga, P.-A. Soderstrom, T. Sumikama, H. Suzuki, R. Taniuchi, Y. Utsuno, J. J. Valiente-Dobon, and K. Yoneda, “Evidence for a new nuclear ‘magic number’ from the level structure of  $^{54}\text{Ca}$ ,” *Nature* **502**, 207–210 (2013).
- [19] M. Rosenbusch, P. Ascher, D. Atanasov, C. Barbieri, D. Beck, K. Blaum, Ch. Borgmann, M. Breitenfeldt, R. B. Cakirli, A. Cipollone, S. George, F. Herfurth, M. Kowalska, S. Kreim, D. Lunney, V. Manea, P. Navrátil, D. Neidherr, L. Schweikhard, V. Somà, J. Stanja, F. Wienholtz, R. N. Wolf, and K. Zuber, “Probing the  $n = 32$  shell closure below the magic proton number  $z = 20$ : Mass measurements of the exotic isotopes  $^{52,53}\text{K}$ ,” *Phys. Rev. Lett.* **114**, 202501 (2015).
- [20] R. F. Garcia Ruiz, M. L. Bissell, K. Blaum, A. Ekström, N. Frömmgen, G. Hagen, M. Hammen, K. Hebeler, J. D. Holt, G. R. Jansen, M. Kowalska, K. Kreim, W. Nazarewicz, R. Neugart, G. Neyens, W. Nörtershäuser, T. Papenbrock, J. Papuga, A. Schwenk, J. Simonis, K. A. Wendt, and D. T. Yordanov, “Unexpectedly large charge radii of neutron-rich calcium isotopes,” *Nature Physics* (2016), 10.1038/nphys3645, 1602.07906.
- [21] D. Seweryniak, M. P. Carpenter, S. Gros, A. A. Hecht, N. Hoteling, R. V. F. Janssens, T. L. Khoo, T. Lauritsen, C. J. Lister, G. Lotay, D. Peterson, A. P. Robinson, W. B. Walters, X. Wang, P. J. Woods, and S. Zhu, “Single-neutron states in  $^{101}\text{Sn}$ ,” *Phys. Rev. Lett.* **99**, 022504 (2007).
- [22] I. G. Darby, R. K. Grzywacz, J. C. Batchelder, C. R. Bingham, L. Cartegni, C. J. Gross, M. Hjorth-Jensen, D. T. Joss, S. N. Liddick, W. Nazarewicz, S. Padgett, R. D. Page, T. Papenbrock, M. M. Rajabali, J. Rotureau, and K. P. Rykaczewski, “Orbital dependent nucleonic pairing in the lightest known isotopes of tin,” *Phys. Rev. Lett.* **105**, 162502 (2010).
- [23] K. L. Jones, A. S. Adekola, D. W. Bardayan, J. C. Blackmon, K. Y. Chae, K. A. Chipps, J. A. Cizewski, L. Erikson, C. Harlin, R. Hatarik, R. Kapler, R. L. Kozub, J. F. Liang, R. Livesay, Z. Ma, B. H. Moazen, C. D. Nesaraja, F. M. Nunes, S. D. Pain, N. P. Patterson, D. Shapira, J. F. Shriner, M. S. Smith, T. P. Swan, and J. S. Thomas, *Nature* **465**, 454–457 (2010).
- [24] J. M. Daugas, R. Grzywacz, M. Lewitowicz, L. Achouri, J. C. Angélique, D. Baiborodin, K. Bennaceur, R. Bentida, R. Béraud, C. Borcea, C. Bingham, W. N. Catford, A. Emsallem, G. de France, H. Grawe, K. L. Jones, R. C. Lemmon, M. J. Lopez Jimenez, F. Nowacki, F. de Oliveira Santos, M. Pfützner, P. H. Regan, K. Rykaczewski, J. E. Sauvestre, M. Sawicka, G. Sletten, and M. Stanoiu, “The  $8+$  isomer in  $^{78}\text{Zn}$  and the doubly magic character of  $^{78}\text{Ni}$ ,” *Phys. Lett. B* **476**, 213 – 218 (2000).
- [25] P. T. Hosmer, H. Schatz, A. Aprahamian, O. Arndt, R. R. C. Clement, A. Estrade, K.-L. Kratz, S. N. Liddick, P. F. Mantica, W. F. Mueller, F. Montes, A. C. Morton, M. Ouellette, E. Pellegrini, B. Pfeiffer, P. Reeder, P. Santi, M. Steiner, A. Stolz, B. E. Tomlin, W. B. Walters, and A. Wöhr, “Half-life of the doubly magic  $r$ -process nucleus  $^{78}\text{Ni}$ ,” *Phys. Rev. Lett.* **94**, 112501 (2005).
- [26] C. Mazzocchi, R. Grzywacz, J.C. Batchelder, C.R. Bingham, D. Fong, J.H. Hamilton, J.K. Hwang, M. Karny, W. Krolas, S.N. Liddick, A.F. Lisetskiy, A.C. Morton, P.F. Mantica, W.F. Mueller, K.P. Rykaczewski, M. Steiner, A. Stolz, and J.A. Winger, “Low energy structure of even-even Ni isotopes close to  $^{78}\text{Ni}$ ,” *Physics Letters B* **622**, 45 – 54 (2005).
- [27] J. Hakala, S. Rahaman, V.-V. Elomaa, T. Eronen, U. Hager, A. Jokinen, A. Kankainen, I. D. Moore, H. Penttilä, S. Rinta-Antila, J. Rissanen, A. Saastamoinen, T. Sonoda, C. Weber, and J. Äystö, “Evolution of the  $n = 50$  shell gap energy towards  $^{78}\text{Ni}$ ,” *Phys. Rev.*

- Lett. **101**, 052502 (2008).
- [28] M. M. Rajabali, R. Grzywacz, S. N. Liddick, C. Maz-zocchi, J. C. Batchelder, T. Baumann, C. R. Bingham, I. G. Darby, T. N. Ginter, S. V. Ilyushkin, M. Karny, W. Królas, P. F. Mantica, K. Miernik, M. Pfützner, K. P. Rykaczewski, D. Weisshaar, and J. A. Winger, “ $\beta$  decay of  $^{71,73}\text{Co}$ : Probing single-particle states approaching doubly magic  $^{78}\text{Ni}$ ,” Phys. Rev. C **85**, 034326 (2012).
  - [29] K. Sieja and F. Nowacki, “Three-body forces and persistence of spin-orbit shell gaps in medium-mass nuclei: Toward the doubly magic  $^{78}\text{Ni}$ ,” Phys. Rev. C **85**, 051301 (2012).
  - [30] Yusuke Tsunoda, Takaharu Otsuka, Noritaka Shimizu, Michio Honma, and Yutaka Utsuno, “Novel shape evolution in exotic Ni isotopes and configuration-dependent shell structure,” Phys. Rev. C **89**, 031301 (2014).
  - [31] V. Somà, C. Barbieri, and T. Duguet, “*Ab initio* gorkov-green’s function calculations of open-shell nuclei,” Phys. Rev. C **87**, 011303 (2013).
  - [32] H. Hergert, S. K. Bogner, T. D. Morris, S. Binder, A. Calci, J. Langhammer, and R. Roth, “*Ab initio* multireference in-medium similarity renormalization group calculations of even calcium and nickel isotopes,” Phys. Rev. C **90**, 041302 (2014).
  - [33] K. Hebeler, S. K. Bogner, R. J. Furnstahl, A. Nogga, and A. Schwenk, “Improved nuclear matter calculations from chiral low-momentum interactions,” Phys. Rev. C **83**, 031301 (2011).
  - [34] A. Ekström, G. R. Jansen, K. A. Wendt, G. Hagen, T. Papenbrock, B. D. Carlsson, C. Forssén, M. Hjorth-Jensen, P. Navrátil, and W. Nazarewicz, “Accurate nuclear radii and binding energies from a chiral interaction,” Phys. Rev. C **91**, 051301 (2015).
  - [35] U. van Kolck, “Few-nucleon forces from chiral Lagrangians,” Phys. Rev. C **49**, 2932–2941 (1994).
  - [36] E. Epelbaum, H.-W. Hammer, and Ulf-G. Meißner, “Modern theory of nuclear forces,” Rev. Mod. Phys. **81**, 1773–1825 (2009).
  - [37] R. Machleidt and D. R. Entem, “Chiral effective field theory and nuclear forces,” Phys. Rep. **503**, 1 – 75 (2011).
  - [38] E. Epelbaum, A. Nogga, W. Glöckle, H. Kamada, Ulf-G. Meißner, and H. Witała, “Three-nucleon forces from chiral effective field theory,” Phys. Rev. C **66**, 064001 (2002).
  - [39] K. Hebeler, H. Krebs, E. Epelbaum, J. Golak, and R. Skibiński, “Efficient calculation of chiral three-nucleon forces up to  $n^3\text{LO}$  for *ab initio* studies,” Phys. Rev. C **91**, 044001 (2015).
  - [40] G. Hagen, A. Ekström, C. Forssén, G. R. Jansen, W. Nazarewicz, T. Papenbrock, K. A. Wendt, S. Bacca, N. Barnea, B. Carlsson, C. Drischler, K. Hebeler, M. Hjorth-Jensen, M. Miorelli, G. Orlandini, A. Schwenk, and J. Simonis, “Neutron and weak-charge distributions of the  $^{48}\text{Ca}$  nucleus,” Nature Physics **12**, 186 (2016).
  - [41] T. Berggren, “On the use of resonant states in eigenfunction expansions of scattering and reaction amplitudes,” Nucl. Phys. A **109**, 265 – 287 (1968).
  - [42] T. Berggren, “On the treatment of resonant final states in direct reactions,” Nucl. Phys. A **169**, 353 – 362 (1971).
  - [43] P. Lind, “Completeness relations and resonant state expansions,” Phys. Rev. C **47**, 1903–1920 (1993).
  - [44] N. Michel, W. Nazarewicz, M. Płoszajczak, and K. Ben-naceur, “Gamow shell model description of neutron-rich nuclei,” Phys. Rev. Lett. **89**, 042502 (2002).
  - [45] R. Id Betan, R. J. Liotta, N. Sandulescu, and T. Vertse, “Two-particle resonant states in a many-body mean field,” Phys. Rev. Lett. **89**, 042501 (2002).
  - [46] G. Hagen, D. J. Dean, M. Hjorth-Jensen, and T. Papenbrock, “Complex coupled-cluster approach to an *ab initio* description of open quantum systems,” Phys. Lett. B **656**, 169 – 173 (2007).
  - [47] F. Coester, “Bound states of a many-particle system,” Nucl. Phys. **7**, 421 – 424 (1958).
  - [48] F. Coester and H. Kümmel, “Short-range correlations in nuclear wave functions,” Nucl. Phys. **17**, 477 – 485 (1960).
  - [49] J. Čížek, “On the Correlation Problem in Atomic and Molecular Systems. Calculation of Wavefunction Components in Ursell-Type Expansion Using Quantum-Field Theoretical Methods,” J. Chem. Phys. **45**, 4256–4266 (1966).
  - [50] H. Kümmel, K. H. Lührmann, and J. G. Zabolitzky, “Many-fermion theory in expS- (or coupled cluster) form,” Physics Reports **36**, 1 – 63 (1978).
  - [51] R. F. Bishop, “An overview of coupled cluster theory and its applications in physics,” Theor. Chim. Acta **80**, 95–148 (1991).
  - [52] B. Mihaila and J. H. Heisenberg, “Microscopic Calculation of the Inclusive Electron Scattering Structure Function in  $^{16}\text{O}$ ,” Phys. Rev. Lett. **84**, 1403–1406 (2000).
  - [53] D. J. Dean and M. Hjorth-Jensen, “Coupled-cluster approach to nuclear physics,” Phys. Rev. C **69**, 054320 (2004).
  - [54] K. Kowalski, D. J. Dean, M. Hjorth-Jensen, T. Papenbrock, and P. Piecuch, “Coupled cluster calculations of ground and excited states of nuclei,” Phys. Rev. Lett. **92**, 132501 (2004).
  - [55] G. Hagen, T. Papenbrock, D. J. Dean, and M. Hjorth-Jensen, “Medium-mass nuclei from chiral nucleon-nucleon interactions,” Phys. Rev. Lett. **101**, 092502 (2008).
  - [56] S. Binder, J. Langhammer, A. Calci, and R. Roth, “*Ab initio* path to heavy nuclei,” Phys. Lett. B **736**, 119 – 123 (2014).
  - [57] R. J. Bartlett and M. Musiał, “Coupled-cluster theory in quantum chemistry,” Rev. Mod. Phys. **79**, 291–352 (2007).
  - [58] G. Hagen, T. Papenbrock, M. Hjorth-Jensen, and D. J. Dean, “Coupled-cluster computations of atomic nuclei,” Rep. Prog. Phys. **77**, 096302 (2014).
  - [59] O. Sorlin, S. Leenhardt, C. Donzaud, J. Duprat, F. Azaiez, F. Nowacki, H. Grawe, Zs. Dombrádi, F. Amorini, A. Astier, D. Baiborodin, M. Belleguic, C. Borcea, C. Bourgeois, D. M. Cullen, Z. Dlouhy, E. Dragulescu, M. Górska, S. Grévy, D. Guillemaud-Mueller, G. Hagemann, B. Herskind, J. Kiener, R. Lemmon, M. Lewitowicz, S. M. Lukyanov, P. Mayet, F. de Oliveira Santos, D. Pantalica, Yu.-E. Penionzhkevich, F. Pougheon, A. Poves, N. Redon, M. G. Saint-Laurent, J. A. Scarpaci, G. Sletten, M. Stanoiu, O. Tarasov, and Ch. Theisen, “ $^{68}\text{Ni}_{40}$ : Magicity versus Superfluidity,” Phys. Rev. Lett. **88**, 092501 (2002).
  - [60] K. Langanke, J. Terasaki, F. Nowacki, D. J. Dean, and W. Nazarewicz, “How magic is the magic  $^{68}\text{Ni}$  nucleus?” Phys. Rev. C **67**, 044314 (2003).
  - [61] S. K. Bogner, R. J. Furnstahl, and R. J. Perry, “Similarity renormalization group for nucleon-nucleon interactions,” Phys. Rev. C **75**, 061001 (2007).



- [62] G. Hagen, M. Hjorth-Jensen, G. R. Jansen, and T. Papenbrock, “Emergent properties of nuclei from ab initio coupled-cluster calculations,” *Physica Scripta* **91**, 063006 (2016).
- [63] B. D. Carlsson, A. Ekström, C. Forssén, D. Fahlin Strömberg, G. R. Jansen, O. Lilja, M. Lindby, B. A. Mattsson, and K. A. Wendt, “Uncertainty analysis and order-by-order optimization of chiral nuclear interactions,” *Phys. Rev. X* **6**, 011019 (2016).
- [64] S. Elhatisari, N. Li, A. Rokash, J. M. Alarcón, D. Du, N. Klein, B.-N. Lu, U.-G. Meißner, E. Epelbaum, H. Krebs, T. A. Lähde, D. Lee, and G. Rupak, “Nuclear binding near a quantum phase transition,” *ArXiv e-prints* (2016), arXiv:1602.04539 [nucl-th].
- [65] N. Michel, W. Nazarewicz, and M. Płoszajczak, “Proton-neutron coupling in the gamow shell model: The lithium chain,” *Phys. Rev. C* **70**, 064313 (2004).
- [66] G. Hagen, T. Papenbrock, D. J. Dean, A. Schwenk, A. Nogga, M. Włoch, and P. Piecuch, “Coupled-cluster theory for three-body Hamiltonians,” *Phys. Rev. C* **76**, 034302 (2007).
- [67] R. Roth, S. Binder, K. Vobig, A. Calci, J. Langhammer, and P. Navrátil, “Medium-Mass Nuclei with Normal-Ordered Chiral  $NN+3N$  Interactions,” *Phys. Rev. Lett.* **109**, 052501 (2012).
- [68] H. Hergert, S. K. Bogner, S. Binder, A. Calci, J. Langhammer, R. Roth, and A. Schwenk, “In-medium similarity renormalization group with chiral two- plus three-nucleon interactions,” *Phys. Rev. C* **87**, 034307 (2013).
- [69] G. R. Jansen, “Spherical coupled-cluster theory for open-shell nuclei,” *Phys. Rev. C* **88**, 024305 (2013).
- [70] A. G. Taube and R. J. Bartlett, “Improving upon ccsd(t): Lambda ccsd(t). i. potential energy surfaces,” *J. Chem. Phys.* **128**, 044110 (2008).
- [71] J. F. Stanton and R. J. Bartlett, “The equation of motion coupledcluster method. a systematic biorthogonal approach to molecular excitation energies, transition probabilities, and excited state properties,” *J. Chem. Phys.* **98**, 7029–7039 (1993).
- [72] J. D. Watts and R. J. Bartlett, “Economical triple excitation equation-of-motion coupled-cluster methods for excitation energies,” *Chem. Phys. Lett.* **233**, 81 – 87 (1995).
- [73] T. J. Watson Jr., V. F. Lotrich, P. G. Szalay, A. Perera, and R. J. Bartlett, “Benchmarking for perturbative triple-excitations in ee-eom-cc methods,” *J. Phys. Chem. A* **117**, 2569–2579 (2013).
- [74] J. R. Gour, P. Piecuch, and M. Włoch, “Active-space equation-of-motion coupled-cluster methods for excited states of radicals and other open-shell systems: Ea-eomccsd and ip-eomccsd,” *J. Chem. Phys.* **123**, 134113 (2005).
- [75] G. R. Jansen, M. Hjorth-Jensen, G. Hagen, and T. Papenbrock, “Toward open-shell nuclei with coupled-cluster theory,” *Phys. Rev. C* **83**, 054306 (2011).
- [76] S.K. Bogner, R.J. Furnstahl, P. Maris, R.J. Perry, A. Schwenk, and J.P. Vary, “Convergence in the no-core shell model with low-momentum two-nucleon interactions,” *Nucl. Phys. A* **801**, 21 – 42 (2008).
- [77] P.-G. Reinhard and W. Nazarewicz, “Information content of a new observable: The case of the nuclear neutron skin,” *Phys. Rev. C* **81**, 051303 (2010).
- [78] L. Platter, H.-W. Hammer, and Ulf-G. Meißner, “On the correlation between the binding energies of the triton and the  $\alpha$ -particle,” *Phys. Lett. B* **607**, 254 – 258 (2005).
- [79] “Supplemental material.”
- [80] R. Taniuchi *et al.*, “in preparation,” (2016).
- [81] G. Hagen, T. Papenbrock, D. J. Dean, M. Hjorth-Jensen, and B. Velamuri Asokan, “*Ab initio* computation of neutron-rich oxygen isotopes,” *Phys. Rev. C* **80**, 021306 (2009).
- [82] E. Khan, N. Paar, and D. Vretenar, “Low-energy monopole strength in exotic nickel isotopes,” *Phys. Rev. C* **84**, 051301 (2011).
- [83] P. Ring and P. Schuck, *The Nuclear Many-Body Problem* (Springer, Heidelberg, 1980).
- [84] M. Wang, G. Audi, A. H. Wapstra, F. G. Kondev, M. MacCormick, X. Xu, and B. Pfeiffer, “The AME2012 atomic mass evaluation,” *Chin. Phys. C* **36**, 1603 (2012).
- [85] G. Hagen, P. Hagen, H.-W. Hammer, and L. Platter, “Efimov physics around the neutron-rich  $^{60}\text{Ca}$  isotope,” *Phys. Rev. Lett.* **111**, 132501 (2013).
- [86] J. Erler, N. Birge, M. Kortelainen, W. Nazarewicz, E. Olsen, A. M. Perhac, and M. Stoitsov, “The limits of the nuclear landscape,” *Nature* **486**, 509 – 512 (2012).